

A List of Bright Interferometric Calibrators measured at the ESO VLTI ^{*}

A. Richichi¹ † and I. Percheron¹ and J. Davis²

¹*European Southern Observatory, Karl-Schwarzschildstr. 2, D-85748 Garching bei München, Germany*

²*Sydney Institute for Astronomy, School of Physics, University of Sydney, NSW 2006, Australia*

Accepted 2009 June 19. Received 2009 June 18; in original form 2008 June 9

ABSTRACT

In a previous publication (Richichi & Percheron 2005) we described a program of observations of candidate calibrator stars at the ESO Very Large Telescope Interferometer (VLTI), and presented the main results from a statistical point of view. In the present paper, we concentrate on establishing a new homogeneous group of bright interferometric calibrators, based entirely on publicly available K-band VLTI observations carried out with the VINCI instrument up to July 2004. For this, we have defined a number of selection criteria for the quality and volume of the observations, and we have accordingly selected a list of 17 primary and 47 secondary calibrators. We have developed an approach to a robust global fit for the angular diameters using the whole volume of quality-controlled data, largely independent of a priori assumptions. Our results have been compared with direct measurements, and indirect estimates based on spectrophotometric methods, and general agreement is found within the combined uncertainties. The stars in our list cover the range $K = -2.9$ to $+3.0$ mag in brightness, and 1.3 to 20.5 milliarcseconds in uniform-disk diameter. The relative accuracy of the angular diameter values is on average 0.4% and 2% for the primary and secondary calibrators respectively. Our calibrators are well suited for interferometric observations in the near-infrared on baselines between ≈ 20 m and ≈ 200 m, and their accuracy is superior, at least for the primary calibrators, to other similar catalogues. Therefore, the present list of calibrators has the potential to lead to significantly improved interferometric scientific results.

Key words: Techniques: high angular resolution – Techniques: interferometric – Catalogues – Stars: fundamental parameters

1 INTRODUCTION

Optical long-baseline interferometry (OLBI) is the most powerful technique available to overcome the limitations in angular resolution imposed by the atmosphere, and by the diffraction limit of even the largest and most perfect single mirror telescopes. By combining the light from two or more telescopes separated by distances much larger than the size of their mirrors, OLBI can achieve angular resolutions at the level of one milliarcsecond (mas) or less at optical and near-IR wavelengths. For illustration, 80 m will suffice to completely resolve a 1 milliarcsecond star at H_α , while about 300 m will be required in the K band. The astrophysical advantages of OLBI, as well as its challenging technical difficulties, are described in reviews such as those

by Quirrenbach (2001) and Monnier et al. (2003), and in the large lists of references they contain.

We do not detail here the numerous technical problems related to the difficulty of performing high precision measurements while maintaining an equal optical path between various telescopes. However, we note that a major limitation of OLBI is the need to compare each measurement of a given science target with a similar measurement of a star with known characteristics of angular diameter and spectrum, made as close as possible in time and angular distance. This process of calibration is necessary to correct for the reduction in fringe visibility resulting from instrumental effects and from the wavefront distortions caused by the turbulent atmosphere. The calibration factor is often called the transfer function, and can be expressed as

$$\text{TF} = V^2/V_t^2 \quad (1)$$

where V^2 represents the observed visibility squared, and V_t^2 is the theoretical visibility squared expected for an obser-

^{*} Based on observations made with ESO telescopes at Paranal Observatory

† E-mail: arichich@eso.org

vation without degradation due to instrumental or atmospheric effects for the given source, baseline, and wavelength of observation. Note that here, and in the rest of the paper, we refer to visibility squared as the squared modulus of the complex visibility.

Without entering into the merits and difficulties of obtaining a reliable determination of V^2 , it is clear that the factor TF, and hence the final interferometric measurement, can only be as accurate as our knowledge of the theoretical visibility V_t^2 . This is ultimately defined by the accuracy with which we know the angular diameter of the calibrator star - as well as other characteristics such as its spectrum, which affects the effective wavelength of the observation, and its limb darkening.

There are effectively two approaches to the problem of determining the angular diameters of calibrator stars. One can use a combination of spectrophotometric measurements and theoretical predictions to derive empirical estimates. This has been done in great detail for example by Cohen et al. (1999), while other authors have subsequently added more refined criteria specifically for interferometric observations (Bordé et al. 2002, Mérand et al. 2005). Recently, Bonneau et al. (2006) have further refined this approach by including information from online databases. Alternatively, one can list all available measurements obtained by angular resolution methods, such as done by Richichi et al. (2005). Obviously, both approaches have their advantages and disadvantages. What is used in practice, at several interferometric facilities around the world, is often a mixture of all available information. This can easily lead to biased results. A bias in the calibrator diameter is automatically reflected in a systematic error on all derived interferometric measurements, including the final scientific results. An extended discussion of calibration errors has been provided by Van Belle et al. (2005). We also mention that one could in principle always find suitably unresolved stars to be used as calibrators (i.e. $V=1$ for all practical purposes), but this has the disadvantage that in general these stars would be considerably fainter than the scientific target and thus cause a loss of quality in the results. In principle it is also possible to avoid the use of calibrators altogether by observing the first minimum in the visibility curve of the scientific target. This was the initial approach by Michelson, however it presents the disadvantage that it can only be used for sources which are completely resolved and it involves a number of complications that make it not really suitable for modern, high-precision measurements. We note however that, when using baselines with a significant E-W component, the variation of the visibility with hour angle has the potential to determine an angular diameter without reference to an overall multiplicative factor. This can be used in principle to remove ambiguities in the simultaneous determination of the angular diameters of several stars from the same data set, as is the case in the present work.

In this paper, we derive a new homogeneous list of interferometric calibrators, based on observations collected solely with the ESO Very Large Telescope Interferometer (VLTI, Glindemann et al. 2003). This is among the first attempts of its kind. Van Belle et al. (2008) have recently published an investigation of archival observations from the PTI, also carried out with the goal of establishing a list of calibrators. However, their approach differs from ours in that it is based

primarily on the statistical properties of the observed visibilities and is restricted to essentially unresolved stars whereas the main goal of our work has been to provide a list of consistent and accurate angular diameter measurements. The fact that the PTI and the VLTI are in different hemispheres suggests that the lists of calibrators will be to a large extent complementary. At present we do not have access to the PTI list to establish what is expected to be a minimal overlap. For our goal, we have started from the large volume of VLTI commissioning data collected with the VINCI instrument for candidate calibrator stars (as described in Richichi & Percheron 2005, Paper I hereafter), and we have sought a self-consistent solution. The benefits of this approach are a) the use of a single instrument and facility, with a well understood behaviour in terms of optical and mechanical characteristics; b) the use of a single automated process for the data reduction; and c) relative freedom from possible bias due to poor or wrong input values for the candidate calibrators.

In Sect. 2 we recall the nature of the observations, we provide details of the criteria used to select primary and secondary calibrators, and we discuss our assumptions on the TF stability. In Sect. 3 we describe two different approaches to the global data analysis, while in Sect. 4 we discuss the results obtained for both primary and secondary calibrators, also in the light of other available estimates and direct measurements. We conclude by discussing the merits of this list and provide advice for its use, as well as outlining possible improvements.

2 DEFINITIONS FOR A HOMOGENEOUS, SELF-CONTAINED LIST OF CALIBRATORS

2.1 Data sets and initial selection

The data used in this paper, as well as in Paper I, are extracted from the large volume of VLTI public releases of VINCI data. We have chosen them because of their large number, of the relative simplicity of the VINCI instrument which was designed to combine two telescopes at a time in the undispersed K-band (about 2 to 2.4 μm FWHM), and of the availability of an automated pipeline which produces science-grade results (Ballester et al. 2004, Kervella et al. 2004b). We mention that we used the fiber-optics version of VINCI, i.e. the most commonly used. Other versions using integrated optics were also briefly used. VINCI is now decommissioned.

In the VLTI scheme, the data are divided into observation blocks (OBs). Each OB with VINCI contains a number of scans of the source, typically 250. As reported in Paper I, a total of 18352 VINCI OBs have been made publicly available up to July 2004, covering 688 nights and involving 11 different baseline configurations using both the fixed 8.2 m unit telescopes (UT) and the relocatable 40 cm siderostats. Thanks to the VLTI design, and to the adoption of optimized choices of parameters in the data reduction pipeline, the results from the two sets of telescopes can be considered homogeneous and we make no distinction between them. From Paper I it can be seen that the baselines span the range 8-140 m, and that they have a wide range of position angles with some emphasis on E-W directions.

Table 1. Selection criteria for primary and secondary calibrators

Criterion	Primary	Secondary
OBs / Night	≥ 3	≥ 3
Nights	≥ 3	≥ 2
Total OBs	≥ 9	≥ 8
Baseline Ratio	≥ 1.5	> 1
Minimum V^2	0.05	0.05
Maximum V^2	0.85	0.85
$\sigma V^2 / V^2$	$\leq 5\%$	$\leq 7.5\%$
$\langle \text{Seeing} \rangle$ / Night	$\leq 1''.2$	$\leq 1''.4$
σSeeing / Night	$\leq 0''.5$	$\leq 0''.5$
Number of Selected Stars	18	47
Total nights	51	121
Total OBs	717	942

The quality estimation criteria and the corresponding results have been described in Paper I. In particular, 12066 OBs on objects classified as candidate calibrators were deemed of sufficient quality. The list of candidate calibrators covered in Paper I included 191 stars, and a corresponding catalogue is available on-line.

In Paper I we defined the term candidate calibrator as a source satisfying a number of criteria concerning its photometric stability, the absence of nearby companions, and a spectral type not subject to either sudden or long-term variability (see also Percheron et al. 2003). For the present purpose, we have further restricted ourselves to those stars believed to have compact atmospheres, to be circularly symmetric, and without wavelength effects in the spectral bandpass of the VINCI instrument other than those attributable to a simple black body energy distribution. We have explicitly excluded from the input list of 191 stars of Paper I the following: supergiants, Cepheids and Miras; stars which are non-circularly symmetric such as rapid rotators; double stars with companions bright and/or close enough to affect the measurement of visibility squared; and variable stars with brightness variations $\gtrsim 0.03$ mag in the V band.

2.2 Definition of primary and secondary calibrators

Not all stars were observed systematically and with comparable accuracy, and we have chosen to apply further selection criteria as detailed in Table 1. The criteria are linked with a logical AND. We have defined a list of primary calibrators, for which we have imposed stringent quality criteria and also a high number of repeated observations in the same night and across the whole period under consideration. In parallel, we have established a list of secondary calibrators, where the quality criteria have been relaxed to some extent and for which the frequency and distribution of observations (both in terms of dates and baselines) are less stringent.

The baseline ratio is the ratio between the maximum and minimum projected baseline length with which observations were collected for the same star, and has been introduced to ensure a sufficient span in the sampling of the visibility, at least for the primary calibrators. In turn this provides a critical check on the fit to the assumed model and allows possible discrepancies to be identified. Note that

in some cases the constraint of 1.5 for the baseline ratio among the primary calibrators had to be partly relaxed after a careful check, as explained in Sect. 3.1. Minimum and maximum values for the observed visibility squared were imposed. The minimum value was chosen to reject values that might be affected by unknown low level systematic errors or by significant bandwidth smearing (see Appendix A). It also implicitly rejects all measurements carried out beyond the first visibility minimum, thus avoiding possible issues in the fitting process (such as ambiguities in the location of the minimum and effects of limb-darkening). High values of the visibility are important to test the quality of the fit and the possible presence of contributions from other sources in the beam, but at the high end they too can be biased (Kervella et al. (2004b)). For this reason a maximum threshold for the visibility squared was also applied, which in any case is sufficiently high to ensure a careful check of the model.

Table 1 also lists some minimum requirements on the quality of the night. For this, we used as criteria the fractional error of the visibilities squared, as well as the average and the standard deviation of the seeing for each night. The former is a compromise between enforcing some intrinsic quality on each data point, and the need to preserve a statistically meaningful sample. The latter are computed from the DIMM measurements available from the ESO ambient condition database, of which there are generally of the order of a few hundred per night. It should be noted that the DIMM values are in the visible. For a few nights during which the database was not operative, the average of the DIMM measurements recorded at the beginning and end of each VLTI data file were used. In this case, the data available for each night may be significantly restricted, typically to a few tens of points. Finally, there have been nights in which neither approach was available, and in this case the data were rejected. We have not explicitly added criteria on airmass z , because observations at the VLTI are normally constrained in zenith distance: over 75% of the OBs in our sample were observed with $z \leq 1.3$, and 90% with $z \leq 1.5$.

The criteria listed in Table 1 are to some extent subjective, but they are based on extensive experience gained in analysing the total pool of data with a range of combinations of criteria. The set of values chosen represents the best compromise to ensure the selection of a sizable sample of primary calibrators based on observational data of unquestionable quality, and a sample of secondary calibrators of high quality which is sufficiently large to provide satisfactory sky coverage.

Following the applications of these constraints, the number of primary calibrators was reduced to 17 and these are listed in Table 2 (one of the potential primary calibrators, θ Cet, was removed for other reasons as discussed in Sect. 3.1). In Table 2 we provide the most common identifiers, the V and K magnitudes and the spectral class. An effective temperature has been adopted for each star. Under the assumption of a black body, the effective wavelength of the VINCI observation for each OB has been computed and is also listed in Table 2. The computation was based on an instrumental spectral response which includes the properties of the filter, telescopes, interferometer optics, and detector (Davis & Richichi 2003). Baseline uncertainties are estimated to be negligible and have been ignored. The last

four columns of Table 2 report the total number of nights on which each calibrator was observed and the total number of OBs available. The columns marked as ‘Pre’ list the numbers after the pre-selection made by applying the criteria of Table 1. However, additional criteria were subsequently applied, and the final numbers are listed in the columns marked as ‘Fin’. This is discussed in Sect. 3.1. With the same conventions and prescriptions, the list of potential secondary calibrators is shown in Table 3.

2.3 Stability of the transfer function

A crucial assumption in our approach is that the transfer function remained constant throughout each night, i.e. one unique value for each night. A correlation between seeing and transfer function is commonly accepted but quantitative details remain largely unstudied. Work by Davis et al. (2005) has shown that the assumption of a transfer function constant throughout a whole night can be a good approximation at the Paranal site, but this was by no means a comprehensive study. Results by Le Bouquin et al. (2006) have pointed to variability of the transfer function also in Paranal, although under less than ideal seeing conditions. Interestingly, a separate recent study by Le Bouquin et al. (2009) has shown a very stable transfer function. The analysis of a few selected nights by Spaleniak (2007) showed that the stability of the transfer function is not uncommon, but is not guaranteed either. There is no easy solution to this problem, also considering that in general the VLTI calibrator observations for any given night are interleaved with gaps in time which can amount to many hours, and it is necessary to find a viable compromise. By imposing criteria on the average seeing and its variation, we have sought to restrict our sample to nights with good atmospheric conditions. Other parameters which have been shown to correlate well with the transfer function are atmospheric jitter (Colavita 1999), which unfortunately is not readily available for our sample, and coherence time. We have plotted coherence time against seeing for almost the totality of the nights under consideration, and we have found a marked correlation, with only about 4% of the nights showing a long coherence time when the seeing was relatively poor (i.e. seeing seems to be a tighter constraint than coherence time). It should be noted that both these parameters are estimated at visible wavelengths, for a star other than the one observed at the VLTI, and at a location on the Paranal summit which is not coincident with the interferometer. Recently the VLTI has been complemented with a fringe-tracker (FINITO, Corcione 2003) which is already providing accurate results (Spaleniak 2007, Le Bouquin 2008) and will progressively alleviate some of these problems.

3 THE PROBLEM AND ITS SOLUTIONS

Two approaches have been applied to the problem of extracting consistent angular diameters from the available set of observed calibrator data: a) the analysis of the data on a night-by-night basis (NN), and b) a global solution of the entire data set (GS).

In the NN approach, for each night, starting from a set of initial guesses for the angular diameters, the best value

$$\begin{array}{c}
 (n_{1,1}\theta_1), \dots, \dots, (n_{i,1}\theta_i) \Leftrightarrow \text{TF}_1 \Leftrightarrow (n_{1,1}\theta_1^*), \dots, \dots, (n_{i,1}\theta_i^*) \\
 (n_{1,2}\theta_1), \dots, \dots, (n_{i,2}\theta_i) \Leftrightarrow \text{TF}_2 \Leftrightarrow (n_{1,2}\theta_1^*), \dots, \dots, (n_{i,2}\theta_i^*) \\
 \\
 (n_{1,j}\theta_1), \dots, \dots, (n_{i,j}\theta_i) \Leftrightarrow \text{TF}_j \Leftrightarrow (n_{1,j}\theta_1^*), \dots, \dots, (n_{i,j}\theta_i^*) \\
 \Downarrow \qquad \qquad \qquad \Downarrow \\
 \Theta_1, \dots, \dots, \Theta_i
 \end{array}$$

Figure 1. Schematic description of the night-by-night (NN) approach to the determination of revised diameters Θ of i calibrators observed over j nights. The symbol $n_{i,j}$ denotes the number of measurements available per each calibrator and night. The left-to-right arrows indicate processing done independently for each night. The top-to-bottom arrows indicate an averaging process done across all the nights.

of the transfer function that minimises the spread of calibrator observations is determined. This transfer function is then used to determine new calibrator diameters independently of possible values from other nights. Effectively, this corresponds to solving a relatively large number (equal to the number of available nights) of small independent problems. Each of these has few unknowns, namely the angular diameters of the calibrators observed on the given night. The number of unknowns varied from a minimum of three to a maximum of six for the primary calibrators. At the end of the process, several independent angular diameter determinations are available for each calibrator, and the average is computed across all the nights. A schematic description is given in Fig. 1, where we have denoted with θ_i the initial angular diameters of the calibrators, and with θ_i^* the corrected values.

The GS approach, on the other hand, involves the solution of a single problem with many more unknowns (all the individual angular diameters) and equations (all available nights). The starting point is similar to the NN approach, i.e. a set of initial values for the angular diameters is adopted and a best-fitting transfer function is determined for each night. However, instead of determining the corresponding revised angular diameters for each night, we retain the calibrated values of visibility squared and merge them for all nights for each calibrator. The angular diameter fit is then made to the merged values of visibility squared to obtain a global value for the angular diameter. The process is then iterated starting with the new set of angular diameters. This is represented schematically in Fig. 2.

Convergence is examined independently for each calibrator by comparing the values of its angular diameter θ_i^k and error $\Delta\theta_i^k$ determined at each global iteration k with the previous one. Changes in the angular diameter are applied until both of the following conditions are satisfied:

$$|\theta_i^k - \theta_i^{k-1}| \leq \beta \Delta\theta_i^k \qquad \chi_i^{2k} < \chi_i^{2k-1} \qquad (2)$$

where β is a factor between zero and unity and χ^2 is computed from the fitted model and the input calibrated visibilities squared and errors for each calibrator. It should be noted that the angular diameters for all calibrators are free at each iteration, and the above constraints only determine when they are actually changed. After some trials, we found that $\beta = 0.5$ was a good compromise ensuring sufficient freedom for variation and, at the same time, limiting the

Table 3. Same as Table 2, for the secondary calibrators.

HR	HD	Star	V	K	Spectral Class	λ_{eff} (μm)	Nights		OBs	
							Pre	Fin	Pre	Fin
37	787	HR 37	5.29	1.86	K4III	2.184	2	2	9	8
248	5112	20 Cet	4.78	1.02	M0III	2.185	7	7	38	38
402	8512	θ Cet	3.60	1.29	K0III	2.184	10	8	32	26
440	9362	δ Phe	3.95	1.63	G9III	2.184	4	1	14	3
509	10700	τ Cet	3.50	1.79	G8V	2.184	6	3	20	11
602	12524	χ Phe	5.16	1.57	K5III	2.185	6	3	39	17
1084	22049	ϵ Eri	3.73	1.78	K2V	2.184	6	6	23	23
1136	23249	δ Eri	3.51	1.62	K0IV	2.184	4	4	17	16
1318	26846	39 Eri A	4.90	2.26	K3III	2.184	2	2	21	21
1652	32831	γ_1 Cae	4.58	1.76	K3III	2.184	8	7	38	34
1663	33042	η_2 Pic	5.06	1.52	K5III	2.185	7	6	34	31
1713	34085	β Ori	0.12	0.21	B8Iab:	2.180	7	5	29	16
1799	35536	HR 1799	5.61	2.13	K5III	2.185	4	4	18	18
1829	36079	β Lep	2.84	0.95	G5II	2.183	5	5	37	37
1834	36167	31 Ori	4.71	0.81	K5III	2.185	3	3	15	15
2311	45018	HR 2311	5.62	1.70	K5III	2.185	2	1	8	3
2478	48433	30 Gem	4.50	1.86	K1III	2.184	2	2	8	8
2503	49161	17 Mon	4.78	1.58	K4III	2.184	4	4	19	19
2574	50778	θ CMa	4.09	0.64	K4III	2.184	4	4	14	14
2693	54605	δ CMa	1.84	0.45	F8Iab:	2.182	2	1	10	4
2736	55865	γ_2 Vol	3.77	1.44	K0III	2.184	3	2	19	13
3046	63744	HR 3046	4.70	2.31	K0III	2.184	3	3	12	12
3845	83618	ι Hya	3.91	0.87	K2.5III	2.184	7	3	29	13
3980	87837	31 Leo	4.38	0.98	K4III	2.184	4	3	20	15
4450	100407	ξ Hya	3.54	1.47	G7III	2.183	3	2	15	9
4526	102461	V918 Cen	5.44	1.38	K5III	2.185	3	2	11	6
4831	110458	HR 4831	4.67	2.23	K0III	2.184	5	2	21	7
5287	123123	π Hya	3.26	0.75	K2III	2.184	3	2	9	6
5340	124897	α Boo	-0.04	-2.91	K1.5III	2.184	4	1	18	3
5381	125932	51 Hya	4.77	1.77	K5III	2.185	2	2	9	9
5487	129502	μ Vir	3.90	3.04	F2III	2.181	2	2	9	9
5513	130157	HR 5513	6.07	2.13	K4/K5III	2.185	4	2	18	9
5526	130694	58 Hya	4.42	1.11	K4III	2.184	4	3	15	12
5705	136422	ϕ_1 Lup	3.58	-0.15	K5III	2.185	5	1	23	6
6229	151249	η Ara	3.78	-0.12	K5III	2.185	2	2	9	9
6630	161892	HR 6630	3.19	0.62	K2III	2.184	2	2	10	10
6862	168592	HR 6862	5.09	1.57	K4.5III	2.185	2	1	8	3
6913	169916	λ Sgr	2.83	0.40	K1IIIb	2.184	6	5	26	21
7234	177716	τ Sgr	3.32	0.59	K1IIIb	2.184	2	1	9	6
7557	187642	α Aql	0.77	0.07	A7V	2.181	4	3	15	12
7584	188154	56 Aql	5.79	1.70	K5III	2.185	7	5	27	21
7635	189319	γ Sge	3.53	-0.23	M0III	2.185	3	3	12	12
7869	196171	α Ind	3.12	0.86	K0IIICNvar...	2.184	6	3	30	12
8080	200914	24 Cap	4.53	0.54	K5/M0III	2.185	14	14	67	67
8679	216032	τ Aqr	4.05	0.22	K5III	2.185	3	2	20	14
8685	216149	HR 8685	5.41	2.10	M0III	2.185	5	4	28	22
8812	218594	88 Aqr	3.66	0.94	K1III	2.184	3	3	10	10

In particular, we identified a small number of discrepant points for some stars and removed them: this was justified when the measured value lay several standard deviations away from the other values for the same star in the same night, and plausible instrumental or observational reasons could be identified. We also required that each night should have at least three primary calibrators observed in order to derive a robust estimate of the transfer function. Finally, we took into consideration the fact that the VLTI transfer function was sometimes low due to understood technical reasons (see Paper I for a discussion). In principle the data for these nights are consistent but, for added confidence in the results,

we excluded nights in which the transfer function was below 0.2. As a result, some OBs and even some nights had to be removed, and one star was dropped from our final list (θ Cet, which was subsequently selected as a secondary calibrator). Finally, we note that as a side-effect of this additional filtering, the constraint on the baseline ratio (see Table 1) could not be preserved in all cases. In particular, for about half of the stars the effective span of baselines covers a ratio of 1.2-1.3 rather than the 1.5 initially specified. For these stars we satisfied ourselves, by inspecting the distribution of visibilities, that the model fit was constrained convincingly and we have retained them.

Table 4. List of the angular diameters for the primary calibrators, based on the night-by-night (NN) approach.

Star	$\theta_{\text{UD}}(\text{mas})$	ρ_{λ}	$\theta_{\text{LD}}(\text{mas})$
ι Cet	3.228 ± 0.046	1.0245	3.307 ± 0.047
β Cet	5.191 ± 0.008	1.0228	5.309 ± 0.008
α Cet	12.007 ± 0.295	1.0297	12.364 ± 0.304
γ Eri	8.654 ± 0.448	1.0293	8.908 ± 0.461
α CMa	5.953 ± 0.082	1.0097	6.011 ± 0.083
α CMi A	5.288 ± 0.077	1.0151	5.368 ± 0.078
α Hya	9.384 ± 0.242	1.0258	9.626 ± 0.248
V337 Car	5.245 ± 0.046	1.0264	5.383 ± 0.047
ν Hya	4.489 ± 0.012	1.0254	4.603 ± 0.012
HR 4546	2.473 ± 0.011	1.0258	2.537 ± 0.011
ϵ Crv	4.901 ± 0.045	1.0254	5.025 ± 0.046
θ Cen	5.412 ± 0.066	1.0229	5.536 ± 0.068
χ Sco	2.117 ± 0.031	1.0255	2.171 ± 0.032
δ Oph	9.642 ± 0.067	1.0293	9.925 ± 0.069
ϵ Sco	5.640 ± 0.019	1.0239	5.775 ± 0.019
70 Aql	3.259 ± 0.094	1.0281	3.351 ± 0.097
λ Gru	2.619 ± 0.094	1.0258	2.687 ± 0.096

Table 5. List of the angular diameters for the primary calibrators, based on the global solution (GS) approach. The error for α CMa has been doubled, to account for bandwidth smearing which is described in the Appendix.

Star	$\theta_{\text{UD}}(\text{mas})$	$\theta_{\text{LD}}(\text{mas})$	$\theta_{\text{UD}}^{\text{GS}} - \theta_{\text{UD}}^{\text{NN}}$
ι Cet	3.245 ± 0.010	3.325 ± 0.010	+0.017
β Cet	5.210 ± 0.005	5.329 ± 0.005	+0.019
α Cet	12.216 ± 0.075	12.579 ± 0.078	+0.209
γ Eri	8.389 ± 0.076	8.634 ± 0.078	-0.265
α CMa	6.030 ± 0.020	6.089 ± 0.020	+0.077
α CMi A	5.357 ± 0.023	5.438 ± 0.023	+0.069
α Hya	9.100 ± 0.016	9.335 ± 0.016	-0.284
V337 Car	5.270 ± 0.024	5.409 ± 0.025	+0.025
ν Hya	4.537 ± 0.014	4.652 ± 0.015	+0.048
HR 4546	2.475 ± 0.004	2.538 ± 0.004	+0.002
ϵ Crv	4.897 ± 0.009	5.021 ± 0.010	-0.005
θ Cen	5.431 ± 0.004	5.556 ± 0.005	+0.019
χ Sco	2.121 ± 0.013	2.176 ± 0.013	+0.004
δ Oph	9.663 ± 0.013	9.946 ± 0.013	+0.021
ϵ Sco	5.612 ± 0.008	5.747 ± 0.008	-0.028
70 Aql	3.246 ± 0.014	3.337 ± 0.014	-0.013
λ Gru	2.635 ± 0.020	2.703 ± 0.020	+0.016

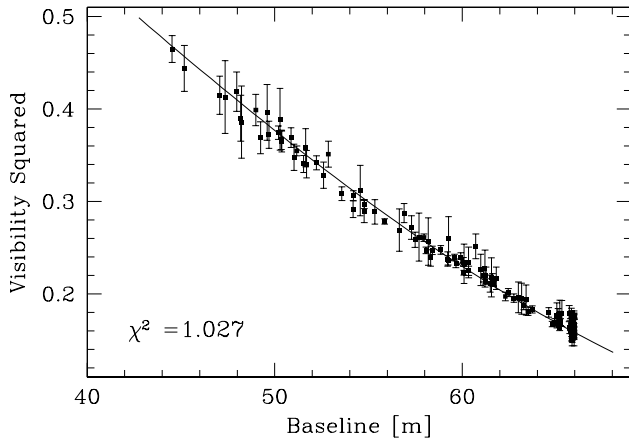


Figure 4. The data set of the star θ Cen, for the total of 21 nights available, analyzed in the global solution (GS) approach. The solid line is the fit for a uniform-disk diameter of 5.431 mas. The normalized χ^2 is indicated.

Subsequently, we applied the GS algorithm, using the NN values given in Table 4 as a starting point. Fig. 4 shows one example of how the GS approach extends over all the available data and nights, and should be compared with Fig. 3. The resulting uniform-disk angular diameter values are listed in Table 5 together with the differences between the GS and NN values. The limb-darkened angular diameters, obtained using the ρ_{λ} coefficients listed in Table 4, are also listed in Table 5.

The differences between the NN and GS results are small, both in absolute and relative terms, confirming that the input values from the NN approach were already quite accurate. The average of the last column in Table 5 is 4 microarcseconds, indicating that there is no systematic bias towards larger or smaller angular diameters between the two approaches.

3.2 Analysis of the secondary calibrators

For the secondary calibrators (SCs hereafter), the GS approach was employed directly; the data set consisted of one squared visibility amplitude for every OB, and were fit with one stellar diameter for each SC and one TF for each night. In applying the GS approach to the SCs, we used both the primary and secondary calibrators available on each night. The PC diameters were fixed with the values of Table 5, and only the SC diameters were free to vary according to the criteria of Eq. 2. While for the primary calibrators (PCs hereafter) we used the NN approach to obtain a set of good starting values for the angular diameters, for the SCs this was not always possible. In addition to a relatively more relaxed set of constraints (see Table 1) for the SCs, we chose to select nights with 2 or more SCs present, rather than the 3 or more for PCs. With only 2 SCs, the NN approach is susceptible to being less reliable than for the case of 3 PCs. A wrong starting value for one of 2 SCs would affect the computed transfer function and, if the SC was only observed on one night (or a very few) with only one other calibrator paired with it, an erroneous final value could result. With 3 PCs, such a situation would have been automatically corrected and, furthermore, the PCs were observed systematically on more nights than the SCs.

A run of the GS approach gave results for the SCs that initially looked convincing but, when it was run again with initial diameters changed by random amounts, it was found that the solutions differed from those of the first run by more than the formal errors on the diameters. Therefore, in the case of the SCs, the robustness of the solution needed further investigation. A large number of simulations, in a MonteCarlo-style (MC) fashion, were undertaken. For this, about 350 loops of the GS were executed. At each loop, the initial diameter guesses were changed by random amounts from the nominal values. The range of changes was set arbitrarily to $\pm 7\%$ of the diameters. Each loop produced vectors of angular diameter and error, one for each SC. From all the

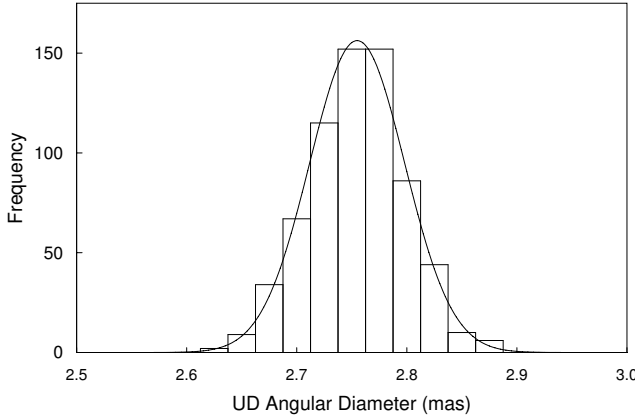


Figure 5. Result of the second and final MC analysis for one of our secondary calibrators, θ Cet. The histogram represents the frequency of solutions obtained from 739 loops of the GS approach, each with random and independent starting values. The line is a Gaussian fit, with average and standard deviation 2.755 mas and 0.043 mas, respectively.

loops, the averages and standard deviations of the angular diameters were deduced based on the hypothesis of a Gaussian distribution of the results. Note that the MC errors were dominant with respect to the formal errors from a typical single GS run.

After this first run, it was realized that for a few sources the fixed range of $\pm 7\%$ was not sufficient to sample the wings of the diameter distribution, and a second run (using the results of the first run as input) was performed. For the second run it was decided to adopt a range of random input values between ± 3 and ± 10 times the formal accuracy of the diameter as derived from the first run, depending on the star. A total of about 750 loops were performed. An example of the distribution of resulting diameters from this MC run for one particular star, θ Cet, can be seen in Fig. 5. We then adopted the mean and standard deviation of the fitting Gaussian profiles for the diameters and their errors, and these are listed in Table 6. Although the quality of the results may vary as reflected by the errors, we note that all the MC distributions were well fitted by Gaussian distributions.

These simulations only address the convergence of our numerical method; they say nothing about the underlying assumptions and little, if anything about correlations between the derived diameters and TF values. Both could result in errors larger than those quoted here. Note that a global fit to the angular diameters and TF values fails when all baselines are North-South (Mozurkewich, Per. Comm.). For each star, the projected baseline is nearly constant through the night and therefore a decrease of all the TF values cannot be differentiated from an increase of all the stellar diameters. For some stars with an East-West baseline, the projected baseline length can change by nearly a factor of two. This breaks the degeneracy between TF and the angular diameter with the diameter determined from the fractional change of $|V|^2$ through the night while the determination of TF is from its mean value. The problem with East-West baselines is that the projected baseline length correlates with zenith angle. Since the most likely systematic

Table 6. List of the angular diameters for the secondary calibrators.

Star	$\theta_{UD}(\text{mas})$	ρ_λ	$\theta_{LD}(\text{mas})$
HR 37	2.517 ± 0.048	1.0270	2.585 ± 0.049
20 Cet	3.361 ± 0.006	1.0289	3.459 ± 0.006
θ Cet	2.755 ± 0.043	1.0225	2.817 ± 0.044
δ Phe	2.208 ± 0.081	1.0229	2.259 ± 0.083
τ Cet	2.030 ± 0.084	1.0200	2.071 ± 0.086
χ Phe	2.754 ± 0.089	1.0276	2.830 ± 0.092
ϵ Eri	2.081 ± 0.064	1.0220	2.127 ± 0.065
δ Eri	2.307 ± 0.085	1.0225	2.359 ± 0.087
39 Eri A	1.677 ± 0.085	1.0265	1.722 ± 0.087
γ_1 Cae	2.173 ± 0.071	1.0261	2.230 ± 0.073
η_2 Pic	2.700 ± 0.061	1.0276	2.774 ± 0.063
β Ori	2.881 ± 0.177	1.0114	2.914 ± 0.179
HR 1799	2.111 ± 0.087	1.0276	2.169 ± 0.090
β Lep	2.942 ± 0.064	1.0208	3.003 ± 0.066
31 Ori	3.495 ± 0.030	1.0272	3.590 ± 0.031
HR 2311	2.509 ± 0.065	1.0276	2.579 ± 0.067
30 Gem	2.236 ± 0.051	1.0235	2.289 ± 0.052
17 Mon	2.491 ± 0.055	1.0270	2.559 ± 0.057
θ CMa	4.032 ± 0.198	1.0265	4.139 ± 0.204
δ CMa	3.583 ± 0.139	1.0180	3.647 ± 0.141
γ_2 Vol	2.460 ± 0.066	1.0229	2.516 ± 0.067
HR 3046	1.726 ± 0.106	1.0229	1.765 ± 0.108
ι Hya	3.365 ± 0.041	1.0255	3.451 ± 0.042
31 Leo	3.259 ± 0.039	1.0270	3.347 ± 0.040
ξ Hya	2.362 ± 0.039	1.0224	2.415 ± 0.040
V918 Cen	3.000 ± 0.029	1.0276	3.082 ± 0.030
HR 4831	1.782 ± 0.048	1.0229	1.823 ± 0.049
π Hya	3.755 ± 0.028	1.0249	3.849 ± 0.028
α Boo	20.453 ± 0.003	1.0230	20.924 ± 0.003
51 Hya	2.220 ± 0.038	1.0276	2.281 ± 0.039
μ Vir	1.255 ± 0.006	1.0139	1.273 ± 0.006
HR 5513	2.136 ± 0.016	1.0273	2.194 ± 0.016
58 Hya	3.297 ± 0.046	1.0260	3.383 ± 0.048
ϕ_1 Lup	5.609 ± 0.215	1.0276	5.764 ± 0.221
η Ara	5.515 ± 0.179	1.0276	5.667 ± 0.184
HR 6630	4.145 ± 0.054	1.0249	4.248 ± 0.056
HR 6862	2.597 ± 0.037	1.0273	2.668 ± 0.038
λ Sgr	4.176 ± 0.044	1.0235	4.274 ± 0.045
τ Sgr	3.987 ± 0.026	1.0235	4.081 ± 0.027
α Aql	3.300 ± 0.227	1.0139	3.346 ± 0.230
56 Aql	2.692 ± 0.028	1.0276	2.767 ± 0.029
γ Sge	6.010 ± 0.047	1.0289	6.184 ± 0.048
α Ind	3.413 ± 0.105	1.0229	3.491 ± 0.108
24 Cap	4.281 ± 0.007	1.0282	4.401 ± 0.008
τ Aqr	4.874 ± 0.132	1.0276	5.008 ± 0.136
HR 8685	1.957 ± 0.071	1.0289	2.013 ± 0.073
88 Aqr	3.240 ± 0.057	1.0235	3.316 ± 0.059

variation of TF is with zenith angle (through a correlation of seeing with zenith angle), East-West baselines are probably more susceptible to systematic errors in the results. Including skewed baselines breaks this final degeneracy. Therefore it is reasonable to expect that with measurements over a sufficient range of baseline lengths and orientations, this algorithm of fitting for both the angular diameters and TF values should work. As such it will help provide the long-sought solution to the problem of calibrating OLBI data on very long baselines. However, these are still assumptions; the sufficiently detailed simulation needed to address these issues is beyond the scope of this paper.

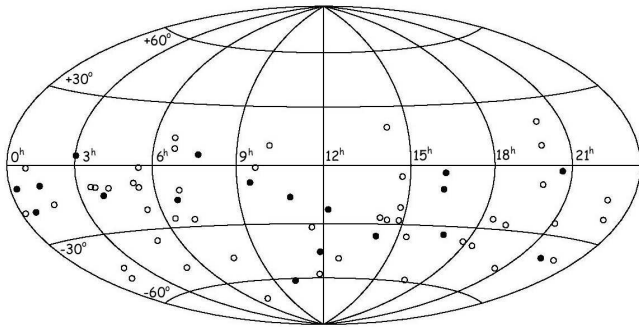


Figure 6. Sky distribution of our primary (solid dots) and secondary (circles) calibrators.

4 RESULTS AND DISCUSSION

The sky coverage of our calibrators is relatively uniform over the range -80° to $+20^\circ$, as shown in Fig. 6. The average distance from any point in the sky, within the above limits in declination i.e. within 45° zenithal distance at Paranal, to one of our calibrators is 11° . Specifically, the average distance to a primary or secondary calibrator is 20° and 13° , respectively.

The angular diameters of the primary calibrators listed in Table 5 have an average accuracy of 0.35%, with the worst case being 0.90%. This constitutes a remarkable achievement for results based on direct observations and internal consistency only. No assumptions were made for any angular diameters except for estimated starting values for the night-by-night approach. In any case, the resulting angular diameters are relatively insensitive to the initial values. A potential systematic effect is associated with the values for the effective wavelengths used in the fitting program. The relative accuracy of 0.35% implies a knowledge of the effective wavelength for each star to better than $0.0077 \mu\text{m}$ and we note that the effective wavelengths were calculated to $0.001 \mu\text{m}$ with an uncertainty of $\pm 0.005 \mu\text{m}$ (Davis & Richichi 2003). An additional uncertainty associated with the limb-darkened angular diameters is the limb-darkening factor discussed in Section 2 but, as pointed out there, the adopted values for T_e , $\log g$, $[\text{Fe}/\text{H}]$ and λ for each star affect the values for the factors at the level of $< 0.1\%$. Any uncertainty associated with the model atmosphere predicted centre-to-limb intensity variations is unknown but is likely to be at a comparable level. The accuracy of the primary calibrator results presented here is superior to most single determinations of angular diameters in published interferometric results and therefore offers significant improvement over what is currently available.

Many of our primary calibrators, being relatively bright, have had values for their angular diameters published either from direct measurements or from indirect estimates. This provides us with the opportunity for a comparison and a check for possible systematic differences. As a first step, we have used the catalogue of Cohen et al. (1999, CC hereafter) which lists limb-darkened angular diameters based on absolutely calibrated stellar spectra, and which has 12 stars in common with our list of primary calibrators. The catalogue of calibrator stars for long baseline stellar interferometry by Bordé et al. (2002, BC hereafter) includes the same 12 stars but adopts the Cohen et al. values for the limb-darkened

Table 7. Comparison of our primary calibrator limb-darkened angular diameters with the values by Cohen et al. (1999). $\Delta\sigma$ expresses the difference in units of the combined error.

Star	VLTI (V)		Cohen (C)		(V - C)	
	θ_{LD} (mas)	σ (mas)	θ_{LD} (mas)	σ (mas)	Δ (mas)	$\Delta\sigma$
ι Cet	3.325	0.010	3.36	0.036	-0.035	-0.9
β Cet	5.329	0.005	5.31	0.055	0.019	0.3
γ Eri	8.634	0.078	8.74	0.088	-0.106	-0.9
V337 Car	5.409	0.025	5.23	0.058	0.179	2.8
ν Hya	4.652	0.015	4.57	0.048	0.082	1.6
HR 4546	2.538	0.004	2.60	0.040	-0.062	-1.5
θ Cen	5.556	0.005	5.46	0.058	0.096	1.6
χ Sco	2.176	0.013	2.10	0.023	0.076	2.9
δ Oph	9.940	0.013	10.03	0.101	-0.090	-0.9
ϵ Sco	5.747	0.008	5.99	0.061	-0.243	-3.9
70 Aql	3.337	0.014	3.27	0.037	0.067	1.7
λ Gru	2.703	0.020	2.71	0.030	-0.007	-0.2
Average					-0.002	0.2

angular diameters and applies limb-darkening corrections to give values for the uniform-disk diameters in a number of spectral bands. The comparison is therefore made with the CC limb-darkened values. The results are listed in Table 7 which lists our values, the CC values, the differences between them in mas, and the differences in units of standard deviations (the latter taken as the sum of the errors from our result and those quoted in CC).

We performed a regression fit of the form $y = ax + b$, where x are our values and y those of CC. Perfect agreement would result in $a = 1$, $b = 0$, and a regression coefficient $R^2 = 1$. The fit gave $a = 1.016 \pm 0.014$, $b = -0.076 \pm 0.077$ and $R^2 = 0.998$. Since the coefficients of the fit are consistent with their expectation values, we conclude that there is no systematic bias and that, for the 12 stars in common, our results and those of CC show very good agreement. On average, the relative accuracy of our results is about 3 times better than those of CC. The fact that the average $|\Delta\sigma|$ is slightly more than unity could be a possible indication of some underestimation of the errors in either of the two samples. We mention that we have performed a detailed comparison also with the UD diameters of BC. Although less compelling because it involves an additional computation from LD to UD performed by the authors, this comparison was also entirely satisfactory. Note that, due to the different range of magnitudes, there is no overlap with the catalogue of Mérand et al. (2005). Other cases of overlap exist between four of the stars in our primary calibrators list and theoretical predictions given in Bell & Gustafsson (1989), Alonso et al. (2000), and Decin et al. (2003). Again there are no systematic differences and, for those cases in which an error in the estimate is quoted by the authors, the difference with our results is less than the sum of the errors (i.e., $\Delta\sigma < 1$ in the sense of Table 7).

A few direct measurements at $2.2 \mu\text{m}$ have been published for four of our primary calibrator stars, and a comparison with our results is provided in Table 8. Again, there is no systematic discrepancy and the differences, in terms of standard deviations as previously defined for Table 7, are

Table 8. Comparison of our primary calibrator diameters with available direct determinations.

Star	UD		LD		Ref.
	Δmas	$\Delta\sigma$	Δmas	$\Delta\sigma$	
α Cet	0.616	1.3			1
α CMa	0.094	2.6	0.050	1.3	2
α CMi A	-0.019	-0.3	-0.010	-0.1	3
δ Oph	-0.417	-0.8			4
	0.363	0.7			5
	0.363	0.9			1

References: 1) Dyck et al. (1996) 2) Kervella et al. (2003) 3) Kervella et al. (2004a) 4) Perrin et al. (1998) 5) Dyck et al. (1998)

generally small. The only possible marginal agreement is with the result by Kervella et al. (2003, K03 hereafter) for α CMa, but even in this case the disagreement is only 1.3 times the combined formal error, when the same quantity is considered, namely the LD diameter. We note that K03 used only one calibrator for their entire set of long-baseline data namely θ Cen, for which they used the diameter estimate from CC. By comparison, our result is based on nights with at least two primary calibrators other than Sirius, and it is not based on any assumptions of angular diameters. Interestingly, the same authors as K03 have obtained an angular diameter for α CMi A, using VINCI and adopting α CMa as the only calibrator, which is in excellent agreement with our value from Table 5.

Several other direct measurements are available for some of our primary calibrators. These include α Cet (Mozurkewich et al. 2003); γ Eri (Mozurkewich et al. 2003); α CMa (Hanbury Brown et al. 1974, Davis & Tango 1986, Mozurkewich et al. 2003); α CMi A (Hanbury Brown et al. 1974, Mozurkewich et al. 2003, Nordgren et al. 2001); α Hya (Mozurkewich et al. 2003); δ Oph (Mozurkewich et al. 2003), as well as SUSI unpublished measurements for α CMa, V337 Car and θ Cen. However these measurements were obtained at a range of wavelengths in the visible and details of band-passes and effective wavelengths are not generally available. For this reason, and since the limb-darkening corrections are larger and possibly more uncertain for visible wavelengths than for $2.2 \mu\text{m}$, we have not made a detailed comparison of derived limb-darkened angular diameters for these results.

Coming to the secondary calibrators, these have lower accuracy on average than the primary ones, as is to be expected from their more relaxed selection criteria. The average accuracy is 2.4%, with ten stars having accuracies better than 1% and five stars between 5% and 7%. Not surprisingly, the smaller stars tend to have the larger uncertainties, although the trend is not very strong and cases of good accuracy can be found throughout the whole range of angular diameters. Almost half of the stars have diameter errors less than 0.05 mas. We have performed the same comparison against CC, as already done for the PCs. Thirty-two of our SCs are in common with CC. The average difference is 0.4σ . A regression fit gives values of $a = 1.032 \pm 0.016$, $b = -0.057 \pm 0.053$ and $R^2 = 0.993$. Fig. 7 illustrates the comparison. Although the agreement is not quite as good as for the PCs it can be regarded nevertheless as satisfactory.

One could endeavour to find possible correlations of the distribution of the differences between our results and

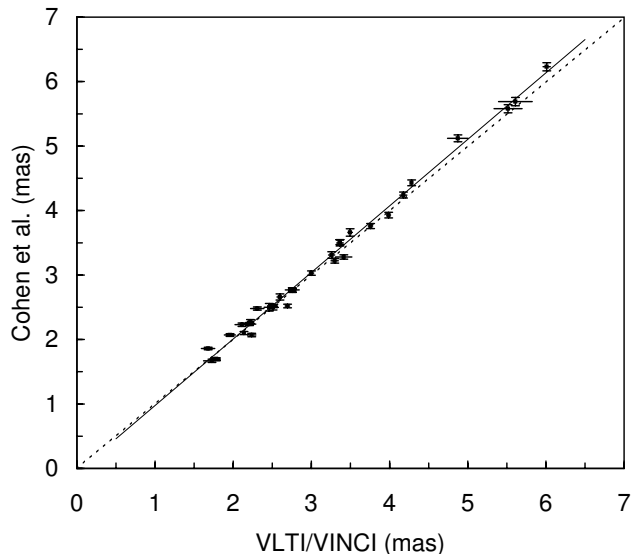


Figure 7. A comparison of our LD angular diameters for the secondary calibrators, against those from the catalogue of Cohen et al. (1999). The dotted line is the 1:1 relationship, and the solid line is a regression fit. Error bars are included but are difficult to be appreciated on this scale.

those of CC, with parameters such as magnitudes or spectral types. However, our sample is rather homogeneous in these respects. About 70% of both primary and secondary calibrators have early K spectral types, and the remainder do not offer sufficient range or statistics to provide significant insight. The same applies for the brightness, which for both types of calibrators are concentrated mostly within 2 magnitudes.

5 CONCLUSIONS

We have undertaken what is probably a unique attempt to derive a homogeneous list of interferometric calibrators, based entirely on observations with the same instrument and without influence from pre-existing estimates. The stars in our list cover a range of magnitudes from ≈ -3 to $\approx +3$ in the K-band, and from 1.3 to 20 mas in diameter. Roughly 70% of the stars have diameters in the 2-5 mas range. Similarly to work done in the area of photometric systems, we have divided our sample into two groups of 17 primary and 47 secondary calibrators. The former have a broader and more detailed database of observations, which has led to a high accuracy and robustness of the results. The primary calibrators have then been used as reference points to help build up the secondary calibrators using a numerical approach to obtain a global solution.

Our calibrators are appropriate for observations in the near-infrared with baselines in the range 20-200 m obtained with aperture sizes in the 1 m class, and as such it can satisfy the needs of most current interferometers. It is clear that, for observations with very long baselines and very large apertures (such as the 8.2 m telescopes of the VLTI), a new approach to interferometric calibration will be needed. This will be necessarily based more on computed diameters than on measured ones. In this case, our calibrators are well

suitable to provide the crucial first step of validating theoretical predictions against measured values. This is especially true in the case of the primary calibrators, with accuracies that provide an exacting test (0.35% on average, 0.9% in the worst case) for theoretical predictions. A comparison with the widely used catalogue of indirect estimates of angular diameters by Cohen et al. (1999), as well as with other similar catalogue and with previous direct measurements when available, gives in general very good agreement. We note however that, at least for the primary calibrators, the internal accuracy achieved in the present work is on average three times better than that of Cohen et al. (1999).

There are some limitations in the present work that must be born in mind. One approximation has been to assume that the transfer function remained constant throughout each night, i.e. one unique value for each night. We have given practical and empirical considerations to justify this choice. The complications involved in the inclusion of variations of the transfer function during the course of each night were beyond the scope of the present study. However, refinements in this approach are indeed important and should be considered in future work wherever feasible.

Another important issue is the correction for limb darkening, which is essential if one wants to relate the angular diameter observed at one wavelength to the work done at another wavelength, or if the diameter is to be used as a parameter in comparisons of observations with stellar atmospheric models. The corrections we have applied are based on model atmosphere predictions of centre-to-limb variations of intensity and they are therefore only as good as the models. However, if improved model predictions become available, our uniform-disk angular diameters remain unchanged and the limb-darkened diameters are readily updated.

ACKNOWLEDGMENTS

This research is based on observations made with the European Southern Observatory telescopes obtained from the ESO/ST-ECF Science Archive Facility, and has made use of the *Simbad* database, operated at the Centre de Données Astronomiques de Strasbourg (CDS), and of NASA's Astrophysics Data System Bibliographic Services (ADS). We acknowledge the detailed comments by the referee Dr. D. Mozurkevich, who has contributed the last paragraph of Sect. 3.2. AR's visits to the School of Physics at the University of Sydney in 2004 and 2006 were supported by an ESO Director General Discretionary Fund grant. JD was a visiting scientist at the ESO Headquarters in Garching during April and May 2005. This work is entirely based on the vast volume of data obtained with the VINCI instrument and made public in the first years of VLTI commissioning. This was made possible through the effort and dedication of a large group of ESO astronomers, engineers and students.

REFERENCES

Alonso A., Salaris M., Arribas S., Martínez-Roger C., Asensio Ramos A. 2000, *A&A*, 355, 1060
 Ballester P., Licha T., McKay D., Percheron I., Peron M. et

al. 2004, *SPIE Proc. Vol. 5493*, Oschmann J.M. Jr. (ed.), p. 16
 Baschek B., Scholz M., Wehrse R. 1991, *A&A*, 246, 374
 Bell R.A., Gustafsson B. 1989, *MNRAS*, 236, 653
 Bonneau D., Clausse J.-M., Delfosse X., Mourard D., Cetre S., Chelli A., Cruzalébes P., Duvert G., Zins G, *A&A*, 456, 789
 Bordé P., Coudé du Foresto V., Chagnon G., Perrin G. 2002, *A&A* 393, 183
 Cayrel de Strobel G., Soubiran C., Friel E.D., Ralite N., Francois P. 1997, *A&ASS*, 124, 299
 Cayrel de Strobel G., Soubiran C., Ralite N. 2001, *A&A*, 373, 159
 Claret A., 2000, *A&A*, 363, 1081
 Cohen M., Walker R.G., Carter B. et al. 1999, *AJ* 117, 1864
 Colavita M.M. 1999, *PASP*, 111, 111
 Davis J., Tango W.J. 1986, *Nature*, 323, 234
 Davis J., Tango W.J., Booth A.J., 2000, *MNRAS*, 318, 387
 Davis J., Richichi A., 2003, *ESO Technical Report VLT-TRE-ESO-15810-3033*
 Davis J., Richichi A., Ballester P. et al. 2005, *AN*, 326, 25
 Decin L., Vandebussche B., Waelkens C., Decin G., Eriksson K., Gustafsson B., Plez B., Sauval A. J. 2003, *A&A*, 400, 709
 Dyck H.M., Benson, J.A., Van Belle, G.T., Ridgway, S.T. 1996, *AJ*, 111, 1705
 Dyck H. M., van Belle G. T., Thompson R. R. 1998, *AJ*, 116, 981
 Corcione L., Bauvier B., Bonino D., Gai M., Gardiol, D. et al. 2003, *GENIE - DARWIN Workshop - Hunting for Planets*, ESO SP-522, p.7.1
 Glindemann, A., Algomedo J., Amestica R., Ballester P., Bauvir B. et al. 2003, *SPIE Proc. Vol. 4838*, Traub W.A. (ed.), p. 89
 Hanbury Brown R., Davis J., Allen L.R. 1974, *MNRAS*, 167, 121
 Kervella P., Thévenin F., Morel P., Bord P., Di Folco E. 2003, *A&A*, 408, 681
 Kervella P., Thévenin F., Morel P., Berthomieu G., Bord P., Provost J. 2004a, *A&A*, 413, 251
 Kervella P., Ségransan D., Coudé du Foresto V. 2004b, *A&A* 425, 1161
 Kurucz R.L. 1993a, *Limbdarkening for 2 km s⁻¹ grid (No.13: [+1.0] to [-1.0])*. Kurucz CD-ROM No. 16
 Kurucz R.L. 1993b, *Limbdarkening for 2 km s⁻¹ grid (No.13: [+0.0] to [-5.0])*. Kurucz CD-ROM No. 17
 LeBouquin J.-B., Labeye P., Malbet F. et al. 2006, *A&A* 450, 1259
 Le Bouquin J.-B., Bauvir B., Haguenaier P., Schöller M., Rantakyro F., Menardi S. 2008, *A&A*, 481, 553
 Le Bouquin J.-B., Bauvir B., Haguenaier P., Schöller M., Rantakyro F., Menardi S. 2008, *A&A*, 481, 553
 Le Bouquin J.-B., Abuter R., Haguenaier P., Bauvir B., Popovic D., Pozna E. 2009, *A&A*, 493, 747
 Mérand A., Bordé P., Coudé du Foresto V. 2005, *A&A* 447, 783
 Monnier J. 2003, *Reports on Progress in Physics*, 66, 789
 Mozurkevich D., Armstrong J.T., Hindsley R.B., Quirrenbach A., Hummel C.A. et al. 2003, *AJ*, 126, 2502
 Nordgren T.E., Sudol J.J., Mozurkevich D. 2001, *AJ*, 122, 2707
 Percheron I., Richichi A., Wittkowski M. 2003, *Astro-*

- physics and Space Science , 286,105
 Perrin G., Coude Du Foresto V., Ridgway S. T., Mariotti J.-M., Traub W. A., Carleton N. P., Lacasse M. G. 1998, A&A, 331, 619
 Quirrenbach A. 2001, Ann. Rev. Astron. Astrophys. 39, 353
 Richichi A., Percheron I. 2002, A&A 386, 492
 Richichi A., Percheron I. 2005, A&A, 434, 1201
 Richichi A., Percheron I., Khristoforova M. 2005, A&A, 431, 773
 Spaleniak I. 2007, ESO Technical Report VLT-TRE-ESO-15830-4411
 Van Belle G.T., Van Belle G. 2005, PASP 117, 1263
 Van Belle, G.T., et al. 2008, ApJSS, 176, 276

APPENDIX A: WAVELENGTH AND BANDPASS ISSUES

In developing a list of interferometric calibrators we are concerned with accuracies in the angular diameters of the order of a few parts in a thousand. At this level, the precise definition of angular diameter as a function of wavelength becomes essential, and in particular it is necessary to account for limb darkening. Similarly, it is crucial to understand in detail the effect of the filter bandpass.

A1 Limb Darkening corrections

The observed visibility values should properly be fitted with the transform for a limb-darkened disk with the centre-to-limb brightness distribution as an additional unknown. However, for stars with compact atmospheres (Baschek et al. 1991), i.e. stars for which the thickness of their atmosphere is very small compared to their radius, the differences between the *shape* of the transform for a uniformly illuminated disk and that for a limb-darkened disk in the region shortward of the first zero in the transform are too small to be measured with sufficient accuracy to distinguish between them reliably. The *scale* of the transform for a limb-darkened disk will differ from that for a uniform-disk depending on the wavelength of observation and on the effective temperature, surface gravity and metallicity of the star. The generally adopted approach is to fit the transform for a uniform-disk to the measurements of visibility squared to obtain the equivalent uniform-disk angular diameter, θ_{UD} , and to apply a correction determined from model stellar atmospheres to obtain a value for the true limb-darkened angular diameter, θ_{LD} . The transform for a uniform-disk is

$$V^2 = \left| \frac{2J_1(\pi b \theta_{UD})}{\lambda_{\text{eff}}} \right|^2 \quad (\text{A1})$$

where J_1 is a Bessel function, b is the projected baseline and λ_{eff} the effective wavelength of observation. Eqn. A1 has been fitted to the observational data to determine values for θ_{UD} . The uniform-disk angular diameters are only applicable for the effective wavelength at which they were measured. For values at other wavelengths the effects of limb-darkening must be taken into account. This generally involves scaling the measured uniform-disk angular diameter to the equivalent limb-darkened angular diameter and then scaling it to the uniform-disk angular diameter for the

desired wavelength. Since the selected primary calibrators are single, non-rotating or slowly rotating stars with compact atmospheres, the limb-darkening scaling factors can be determined from grids of theoretical model stellar atmospheres. Davis et al. (2000) have computed limb-darkening factors ρ_λ as a function of effective temperature (T_e), surface gravity ($\log g$), metallicity ($[\text{Fe}/\text{H}]$) and wavelength (λ) for the entire grid of model atmospheres by Kurucz (1993a,b). Claret (2000) has computed non-linear limb-darkening coefficients for the same model atmospheres and these lead to the same results for the limb-darkening factors. With θ_{UD} the uniform-disk angular diameter at wavelength λ and θ_{LD} the corresponding limb-darkened angular diameter, the limb-darkening factor ρ_λ is defined by

$$\rho_\lambda = \frac{\theta_{LD}}{\theta_{UD}} \quad (\text{A2})$$

In order to obtain the limb-darkening factors we have interpolated within the tabulations given by Davis et al. (2000) with values for T_e , $\log g$, $[\text{Fe}/\text{H}]$ and λ for each star. For λ , the value of the effective wavelength of the measurement (λ_{eff}), as discussed in Section 2.2, was adopted. Values for T_e , $\log g$ and $[\text{Fe}/\text{H}]$ have been obtained for most of the calibrators from the tabulations of Cayrel de Strobel et al. (1997, 2001). For the remaining calibrators, values have been adopted by inspection and interpolation among the values for the other stars. We note that the uncertainties in the adopted values only affect the limb-darkening factors at the level of 0.1%. The values for λ_{eff} and ρ_λ for each star are listed in the Tables 4 and 6. The limb-darkened angular diameters that we list are, following Eqn. A2, the product of the uniform-disk angular diameters and the limb-darkening factors.

A2 Bandwidth smearing

The bandpass of VINCI is 1.92-2.50 μm at the 1% level (Davis & Richichi 2003), and therefore each visibility point is the average, according to proper weights of instrument sensitivity, source spectral distribution and atmospheric transmission, of a wide range of monochromatic visibilities. While this has almost no effect in the linear part of the visibility curve, in the non-linear regime of very low visibility values the broad spectral bandwidth might result in a significant effect on the measured visibilities. There is the further complication that the monochromatic uniform-disk angular diameter will vary across the bandpass. We have performed numerical investigations of this effect for a number of extreme cases among our sample, in particular for the three primary calibrators α CMa, ϵ Crv and V337 Car, and the secondary calibrator V918 Cen. All these objects had some calibrated visibility squared values as low as ≈ 0.1 and were therefore expected to be most sensitive to bandwidth smearing. The differences that we found between the diameter derived from a monochromatic analysis at the assumed effective wavelength, and the diameter derived from a detailed multi-wavelength analysis, were smaller than the formal errors in the diameters. This effect is systematic but it is not necessarily in the same direction as it depends on the baselines used. For stars with only short baseline observations the fitted uniform-disk angular diameters will be too large but, for long baseline observations or a range of baselines in-

cluding long ones, the fitted diameters will be too small. Our investigation showed that the effect of bandwidth smearing could be significant if only low visibility values were used in the angular diameter fitting program. However, in general, observations at several baselines were available for the fitting program giving a combination of high and low visibilities. Only in the case of α CMa was the difference comparable with the formal error. Given these results it was decided to ignore, with considerable simplification of the data analysis, the effect of bandwidth smearing for all stars, and to increase the formal error by a factor of two for α CMa alone.